Yokohama Publishers
ISSN 1349-8169 ONLINE JOURNAL

Pacific Journal of Optimization
Vol. 21, No. 3, pp. 493–518, 2025

TWO-STAGE NUMERICAL METHOD FOR SPARSE SOURCE IDENTIFICATION PROBLEM OF LINEAR DIFFUSION-ADVECTION EQUATIONS*

Hailing Wang, Hansong Yan, Di Wu† and Yanqin Bai

Abstract: This paper addresses a sparse initial source identification problem with linear diffusion-advection equations and a given final time. The problem's complexity arises from the initial source's structure, a linear combination of Dirac measures. Moreover, the strong diffusion and smoothing effects of the linear diffusion-advection equation further render the problem exponentially ill-posed and non-smooth. To overcome these obstacles, we propose a two-stage numerical method. In the first stage, we reformulate the identification problem as a sparse optimal control problem, incorporating L^1 and L^2 regularization terms into the cost function to encourage sparsity and ensure well-posedness. To solve the sparse optimal control problem efficiently, augmented Lagrangian technique is extent to an inexact setting, where the sub-problem in each iteration is addressed using the semi-smooth Newton method. For the large-scale and ill-conditioned Newton system involved, an efficient preconditioned conjugate gradient method is designed. Additionally, we demonstrate that with the appropriate selection of the penalty parameter, the proposed inexact augmented Lagrangian algorithm can achieve super-linear convergence rate. At the second stage, we refine the solution obtained at the first stage into a linear combination of Dirac measures. This process entails a location identification procedure and solving a small-scale least squares fitting problem. Lastly, three types of sparse initial source identification problems are considered and solved to demonstrate the feasibility and effectiveness of the proposed algorithm.

Key words: *sparse source identification, linear diffusion-advection equation, augmented Lagrangian, preconditioner design*

Mathematics Subject Classification: *49M25, 49M29, 90C22*

1 Introduction

Consider the following linear diffusion-advection equation:

$$\begin{cases} \partial_t u - d\Delta u + v \cdot \nabla u = 0, & \text{in} \quad \Omega \times (0,T), \\ u = 0, & \text{on} \quad \Gamma \times (0,T), \\ u(x,0) = u_0(x), & \text{in} \quad \Omega, \end{cases} \tag{1.1}$$

where $\Omega \subseteq \mathbb{R}^n$ represents the space domain, and $\Gamma := \partial\Omega$ denotes the piece-wise continuous boundary of Ω. The parameters include the given terminal time $0 < T < +\infty$, the diffusivity

*This work was supported by the Shanghai Key Laboratory of Pure Mathematics and Mathematical Practice (Grant No. 18dz2271000) and the National Natural Science Foundation of China (NSFC) (Grant Nos. 12171307, 12271335).

†Corresponding author

 DOI: https:// doi.org/10.61208/pjo-2025-024

coefficient $d > 0$ and the velocity of the advection v. The aim of the sparse initial source identification problem is to determine the initial source $u_0(x)$ based on the observation of the terminal state $u_T(x)$. $u_0(x)$ must be composed through a linear combination of Dirac measurements:

$$u_0 = \sum_{i=0}^{l} \alpha_i^* \delta_{x_i}, \tag{1.2}$$

where $\delta_{x_i}(x_i) = 1$ and $\delta_{x_i}(x) = 0$ for any $x \neq x_i$. Sparse initial source identification problem has various practical applications, such as pinpointing point-wise pollution sources [1,14,21] and localizing the release of airborne contaminants [9, 12]. The structure of u_0 and the coupled of the intensities and locations make it hard to be numerically solved. Specifically, the low regularity of u_0 implies that the resulting solution u of (1.1) resides in the space $L^r(0,T;W_0^{1,p}(\Omega))$ with $p, r \in [1,2)$, where $\frac{2}{r} + \frac{n}{p} > n+1$. This characteristic complicates the discretization of the linear diffusion-advection equation and the convergence of proposed numerical methods [8]. Additionally, as noted in [17], the problem is exponentially ill-posed due to diffusive and smoothing effects. Even a slight noise in the observation of $u_T(x)$ can lead to a significant error in the obtained solution. Hence, direct solution of the identification problem is daunting. It is customary to reformulate sparse initial source identification as an optimal control problem involving partial differential equations (PDEs). In this formulation, the initial term is treated as the control variable, and the cost function gauges the disparity between the observation u_T and the corresponding terminal state [3,8,11,22,24].

In [8,11,22], a regularization term $\beta\|u_0\|_{\mathcal{M}(\Omega)}$ is introduced into the objective function to encourage the sparsity of u_0. The problem is then reformulated as:

$$\min_{u_0 \in \mathcal{M}(\Omega)} \frac{1}{2}\|u(\cdot,T) - u_T\|^2_{L^2(\Omega)} + \beta\|u_0\|_{\mathcal{M}(\Omega)}, \tag{1.3}$$

where $u(\cdot,t)$ is the solution of partial differential equation (1.1) corresponding to $u_0(x)$, $\mathcal{M}(\Omega)$ denotes the space of Borel measures in Ω and β is a regularization parameter. It's crucial to highlight that the reformulated problem transforms into a convex optimization problem, showcasing a more advantageous structure compared to the original identification problem. The existence and uniqueness of the solution are established in [8], and under specific assumptions, the resulting solution is additionally shown to conform to the form outlined in (1.2) [22]. However, the presence of the measure valued function brings many difficulties to numerical computation because the measure entails appropriate numerical discretization scheme and prevent the application of some well-developed optimization methods. For example, the semi-smooth Newton (SSN) method can not be applied because the corresponding optimality conditions can not be formulated as semi-smooth equations [16].

To promote the sparsity structure and improve the computation efficiency, $\mathcal{M}$ norm is replaced by L^1 norm [24]. The problem thus becomes

$$\min_{u_0 \in L^1(\Omega)} \frac{1}{2}\|u(\cdot,T) - u_T\|^2_{L^2(\Omega)} + \beta\|u_0\|_{L^1(\Omega)}, \tag{1.4}$$

which is solved by gradient descend method. Given that the optimal solution of problem (1.4) may not satisfy the initial source identification, the approach initially focuses on identifying the location before tackling the least-square fitting problem. Nonetheless, the well-posedness of (1.4) may not be ensured since the function space $L^1(\Omega)$ lacks reflexivity, as deliberated in [16,33]. To address this concern, an extra L^2 regularization term is introduced, thereby relocating the problem to L^2 space, namely,

$$\min_{u_0 \in L^2(\Omega)} \frac{1}{2}\|u(\cdot,T) - u_T\|^2_{L^2(\Omega)} + \beta\|u_0\|_{L^1(\Omega)} + \frac{\tau}{2}\|u_0\|^2_{L^2(\Omega)}. \tag{1.5}$$

It is shown in [7] that under some regularity assumptions the solution of Problem (1.5) converges to that of Problem (1.3) as $\tau \to 0$.

The classical gradient descent method designed in [24] can be extended to tackle Problem (1.5). Subsequently, to enhance efficiency, the primal-dual hybrid gradient descent (PDHG) method is proposed for addressing Problem (1.5) [4]. Numerical findings demonstrate that the proposed algorithm significantly outperforms the gradient descent (GD) method in terms of computational speed. However, the convergence rate of PDHG in a non-ergodic sense is slow, typically of the order $O(1/K)$, where K represents the iteration count. Furthermore, achieving a solution with enhanced sparsity in practical scenarios or a solution closely approximating the one from Problem (1.3) theoretically necessitates a very small regularization parameter τ [7]. Consequently, the regularized Problem (1.5) becomes highly ill-conditioned.

To overcome these challenges, a new two-stage numerical method is designed in this paper for solving the initial source identification problem. In the first stage, we prioritize solving Problem (1.5), as it exhibits better well-posedness in the L^2 space and less ill-conditioning compared to Problem (1.4). We start by separating the smooth and non-smooth L^1 term within the objective functional, transforming Problem (1.5), governed by the partial differential equation (1.1), into an equality-constrained optimal control problem. This transformed problem is then tackled using the inexact augmented Lagrangian (ALM) method. Each iteration involves the application of the semi-smooth Newton method (SSN) to solve each non-smooth but unconstrained sub-problem, with an efficient preconditioned conjugate gradient (PCG) method integrated to expedite the process. Additionally, we establish the convergence of the inexact ALM and achieve a super-linear non-ergodic convergence rate. However, although the solution obtained in the first step demonstrates sparsity, it doesn't conform to the structure outlined in (1.2). Therefore, a structural enhancement is essential in the second stage. Specifically, we identify the optimal positions by finding the maxima of the absolute value of the obtained solution, and then obtain the optimal intensities by minimizing the distance between the terminal source and the observation $u_T(x)$. This step can be attributed to solving a small-scale least-square fitting problem.

The rest of this paper is organized as follows. In Section 2, we provide preliminary insights into the reformulated Problem (1.5), covering aspects such as the existence and uniqueness of the solution, along with the optimality conditions. Section 3 introduces an inexact augmented Lagrangian method (ALM) devised to tackle the transformed problem, incorporating an efficient SSN-PCG method tailored to solve the sub-problems within each iteration of the inexact ALM method. We delve into strategies for enhancing the sparsity structure of the obtained solution in Section 4, leading to the proposal of a two-stage numerical method for addressing the initial source identification problem. Section 5 is dedicated to establishing the convergence and estimating the super-linear convergence rate in the non-ergodic sense for the inexact ALM method. In Section 6, we present and solve three numerical examples, encompassing scenarios involving homogeneous and heterogeneous mediums, coupled models, and noisy observations. Finally, in Section 7, we provide concluding remarks.

2 Preliminaries

Let us reformulate Problem (1.5) as the following optimal control problem (P):

$$\min_{u_0 \in L^2(\Omega)} \quad J(u_0) := \frac{1}{2} \iint_{\Omega} \mid u(x,T) - u_T(x) \mid dx + \frac{\tau}{2} \iint_{\Omega} \mid u_0(x) \mid^2 dx + \beta \iint_{\Omega} \mid u_0(x) \mid dx. \tag{P}$$

For simplicity, we omit the space argument x and denote the inner product and norm of the function space $L^2(\Omega)$ as $\langle\cdot,\cdot\rangle$ and $\|\cdot\|$ in subsequent discussions. It is easy to see that Problem (P) is actually a convex but non-smooth optimal control problem. Then, we have the following existence theorem of the solution and derive the first-order optimality conditions.

Theorem 2.1. *There exists a unique initial state $u_0^* \in L^2(\Omega)$ as the optimal solution of Problem (P), and u_0^* satisfies the following optimality conditions:*

$$0 \in \tau u_0^* + p^*(\cdot,0) + \beta\partial\|u_0^*\|_1, \tag{2.1}$$

where

$$\partial\|u_0^*\|_1 := \begin{cases} 1, & \text{if} \quad u_0^* > 0, \\ \{g \mid -1 \le g \le 1\}, & \text{if} \quad u_0^* = 0, \\ -1, & \text{if} \quad u_0^* < 0, \end{cases}$$

denotes the sub-differential of the functional $\|u_0^*\|_1$, $p^*(\cdot,0)$ is the corresponding adjoint variable p^* at $t=0$ and p^* is the solution of the following PDEs,

$$\begin{cases} \partial_t u - d\Delta u + v\cdot\nabla u = 0, & \text{in} \quad \Omega\times(0,T), \\ u = 0, & \text{on} \quad \Gamma\times(0,T), \\ u(x,0) = u_0(x), & \text{in} \quad \Omega, \end{cases} \tag{2.2}$$

$$\begin{cases} \partial_t p + d\Delta p + v\cdot\nabla p = 0, & \text{in} \quad \Omega\times(0,T), \\ p = 0, & \text{on} \quad \Gamma\times(0,T), \\ p(x,T) = u(x,T) - u_T(x), & \text{in} \quad \Omega. \end{cases} \tag{2.3}$$

Proof. The proof of existence theorem is similar with that for Theorem 1.43 in [16] and the derivation of the first-order optimality conditions is based on the perturbation analysis in [15], and thus is omitted here. □

It is worth noting that the optimality conditions (2.1) reflect the sparsity structure properties of the solution u_0^*, which can be obtained similarly as done in [4, 7, 18].

3 Numerical solution procedure of first stage

3.1 Inexact augmented Lagrangian method

Define the operator $\mathcal{L}$ induced by (1.1) as

$$\mathcal{L}(u_0(x)) := u(x,T \mid u_0(x)), \tag{3.1}$$

and the functionals $f : L^2(\Omega)\to\mathbb{R}$ and $g : L^2(\Omega)\to\mathbb{R}$:

$$f(u_0) := \frac{1}{2}\iint_\Omega \mid \mathcal{L}(u_0) - u_T \mid^2 dx + \frac{\tau}{2}\iint_\Omega \mid u_0 \mid^2 dx, \quad g(u_0) := \beta\iint_\Omega \mid u_0 \mid dx. \tag{3.2}$$

By introducing an auxiliary variable $z \in L^2(\Omega)$, Problem (P) can be further rewritten as Problem $(\tilde{P})$:

$$\begin{aligned} \min_{(u_0,z)^\top \in L^2(\Omega)\times L^2(\Omega)} \quad & f(u_0) + g(z) \\ \text{s.t.} \quad & u_0 = z. \end{aligned} \tag{$\tilde{P}$}$$

Noted that Problem $(\tilde{P})$ has a separable structure. Then, the augmented Lagrangian functional corresponding to Problem $(\tilde{P})$ can be defined by

$$L_\sigma(u_0, z; \lambda) := f(u_0) + g(z) + \langle \lambda, u_0 - z\rangle + \frac{\sigma}{2}\|u_0 - z\|^2, \tag{3.3}$$

where σ is a given penalty parameter. On this basis, we can design an inexact augmented Lagrangian method to solve Problem $(\tilde{P})$ as follows.

Algorithm 1 An inexact ALM for Problem $(\tilde{P})$

Step 1: Let σ_0 be a given parameter, $\{\epsilon_k\}$ be a summable sequence of non-negative numbers, and initialize the multiplier $\lambda^0 \in L^2(\Omega)$.

Step 2: Compute $(u_0^{k+1}, z^{k+1})^\top$ such that

$$e^{k+1} \in \partial L_{\sigma_k}(u^{k+1}, z^{k+1}; \lambda^k) \quad \text{and} \quad \|e^{k+1}\| \le \epsilon_k. \tag{3.4}$$

Step 3: Compute

$$\lambda^{k+1} = \lambda^k + \sigma_k(u_0^{k+1} - z^{k+1}), \tag{3.5}$$

and update the parameter $\sigma_{k+1} \uparrow \sigma_\infty \le +\infty$. Set $k = k + 1$ and return to **Step 2.**

To show the **Step** 2 of Algorithm 1 is implementable, we have the following theorem.

Theorem 3.1. *There exists a unique* $(\bar{u}_0^{k+1}, \bar{z}^{k+1})^\top \in L^2(\Omega)\times L^2(\Omega)$ *as the optimal solution of the following problem,*

$$\min_{(u_0,z)^\top \in L^2(\Omega)\times L^2(\Omega)} L_{\sigma_k}(u_0, z; \lambda^k). \tag{3.6}$$

Proof. The proof of Theorem 3.1 is similar with that of Theorem 1.43 in [16], thus is omitted here. □

Remark 3.2. Theorem 3.1 makes Algorithm 1 well-defined. And if we choose $\epsilon_k = 0$, Algorithm 1 is exactly an ALM method.

We shall discuss how to solve the sub-problem (3.6) in the next two sub-sections.

3.2 Semi-smooth Newton method

Since Theorem 3.1 guarantees the existence and uniqueness of the solution $(\bar{u}_0^{k+1}, \bar{z}^{k+1})$ of sub-problem (3.6), we have

$$Df(\bar{u}_0^{k+1}) + \lambda^k + \sigma_k(\bar{u}_0^{k+1} - \bar{z}^{k+1}) = 0, \tag{3.7}$$

$$0 \in \partial g(\bar{z}^{k+1}) - \lambda^k - \sigma_k(\bar{u}_0^{k+1} - \bar{z}^{k+1}). \tag{3.8}$$

From (3.8), we obtain that

$$\bar{z}^{k+1} = \mathrm{Prox}_{\frac{g}{\sigma_k}}(\bar{u}_0^{k+1} + \frac{\lambda^k}{\sigma_k}), \tag{3.9}$$

where $\mathrm{Prox}_{\frac{g}{\sigma_k}} := (\mathrm{I} + \frac{\partial g}{\sigma_k})^{-1}$ is called the proximal operator corresponding to $\frac{g}{\sigma_k}$. By substituting (3.9) into (3.7), there holds

$$Df(\bar{u}_0^{k+1}) + \sigma_k\left(\bar{u}_0^{k+1} + \frac{\lambda^k}{\sigma_k} - \mathrm{Prox}_{\frac{g}{\sigma_k}}(\bar{u}_0^{k+1} + \frac{\lambda^k}{\sigma_k})\right) = 0. \tag{3.10}$$

Therefore, sub-problem (3.6) can be solved by first solving (3.10) to get $\bar{u}_0^{k+1}$ and then obtain $\bar{z}^{k+1}$ by (3.9).

Based on the perturbation analysis in [15], we derive the first-order differential of the functional $f(\cdot)$ at u_0 given by

$$Df(u_0) = p(\cdot, 0) + \tau u_0, \tag{3.11}$$

where $p(\cdot, 0)$ is the adjoint variable p at $t = 0$ and p is obtained from the following two PDEs,

$$\begin{cases} \partial_t u - d\Delta u + v \cdot \nabla u = 0, & \text{in} \quad \Omega \times (0, T), \\ u = 0, & \text{on} \quad \Gamma \times (0, T), \\ u(x, 0) = u_0(x), & \text{in} \quad \Omega, \end{cases} \tag{3.12}$$

$$\begin{cases} \partial_t p + d\Delta p + v \cdot \nabla p = 0, & \text{in} \quad \Omega \times (0, T), \\ p = 0, & \text{on} \quad \Gamma \times (0, T), \\ p(x, T) = u(x, T) - u_T(x), & \text{in} \quad \Omega. \end{cases} \tag{3.13}$$

On the other hand, according to the definition of $g(\cdot)$ (3.2), there holds

$$\mathrm{Prox}_{\frac{g}{\sigma_k}}(\bar{u}_0^{k+1} + \frac{\lambda^k}{\sigma_k}) = \min\left(\bar{u}_0^{k+1} + \frac{\lambda^k + \beta}{\sigma_k}, 0\right) + \max\left(\bar{u}_0^{k+1} + \frac{\lambda^k - \beta}{\sigma_k}, 0\right). \tag{3.14}$$

Thus, (3.10) is equivalent to

$$p^{k+1}(\cdot, 0) + \tau \bar{u}_0^{k+1} + (\sigma_k \bar{u}_0^{k+1} + \lambda^k) - \min\left(\sigma_k \bar{u}_0^{k+1} + \lambda^k + \beta, 0\right) - \max\left(\sigma_k \bar{u}_0^{k+1} + \lambda^k - \beta, 0\right) = 0,$$

where $p^{k+1}(\cdot, 0)$ is obtained by solving (3.12)-(3.13) with $u_0 = \bar{u}_0^{k+1}$.

In order to represent the equation (3.10) in a compact form, define an operator $\widetilde{\mathcal{L}}$ mapping from the solution at the terminal time to that at the initial time,

$$\widetilde{\mathcal{L}}(p(x, T)) := p(x, 0 \mid p(x, T)),$$

then the solution of (3.13) at $t = 0$ can be represented as $\widetilde{\mathcal{L}}(u(x, T) - u_T(x))$. Furthermore, due to the linearity of $\widetilde{\mathcal{L}}$ and the definition of $\mathcal{L}$ (3.1), we obtain

$$p^{k+1}(x, 0) = \widetilde{\mathcal{L}}(\bar{u}^{k+1}(x, T) - u_T(x)) = \widetilde{\mathcal{L}}(\mathcal{L}(\bar{u}_0^{k+1})) - \widetilde{\mathcal{L}}(u_T).$$

Therefore, (3.10) is equivalent to

$$(\widetilde{\mathcal{L}}\mathcal{L} + \tau \mathrm{I})\bar{u}_0^{k+1} + \sigma_k \bar{u}_0^{k+1} - \min\left(\sigma_k \bar{u}_0^{k+1} + \lambda^k + \beta, 0\right) - \max\left(\sigma_k \bar{u}_0^{k+1} + \lambda^k - \beta, 0\right) = \widetilde{\mathcal{L}}(u_T) - \lambda^k. \tag{3.15}$$

Then we solve the (3.15) by numerical discretization.

We employ the backward-Euler finite difference method with time step Δt for the time discretization ($N = T/\Delta t$), and the piece-wise linear finite element method with mesh size h for the space discretization. Specifically, let $\{\phi_i\}_{i=1}^n$ represent the basis of the finite element space, $M \in \mathbb{R}^{n \times n}$ be the mass matrix, $K \in \mathbb{R}^{n \times n}$ be the matrix corresponding to the discretization of the diffusion term $-d\Delta$ and $A \in \mathbb{R}^{n \times n}$ be the matrix corresponding to the discretization of the advection term $v \cdot \nabla$, precisely,

$$\begin{aligned} &M = (m_{ij})_{n \times n}, \quad m_{ij} = \int_\Omega \phi_i \phi_j dx, \quad K = (k_{ij})_{n \times n}, \quad k_{ij} = \int_\Omega d\nabla \phi_i \cdot \nabla \phi_j dx, \\ &A = (a_{ij})_{n \times n}, \quad a_{ij} = \int_\Omega \phi_i (v \cdot \nabla \phi_j) dx. \end{aligned} \tag{3.16}$$

Let us define $\bar{\boldsymbol{u}} := \{\bar{\boldsymbol{u}}_i\}_{i=0}^N$ where $\bar{\boldsymbol{u}}_i \in \mathbb{R}^n$ is the finite element approximation of the state variable $\bar{u}$ at time $t = i\tau$. The notation $\boldsymbol{\lambda}^k$ is defined in a similar sense for the function λ^k. The notation $\boldsymbol{u}_T$ denotes the finite element approximation of the function $u_T(x)$. Besides, the operator $\mathcal{L}$ is approximated by $\mathcal{L}^d$ in the way of Algorithm 2,

Algorithm 2 Discretize the operator $\mathcal{L}$ as $\mathcal{L}^d$

Input: $\bar{\boldsymbol{u}}_0$ and N
Output: $\bar{\boldsymbol{u}}_N$
1: **for** $i = 1, 2, \ldots, N$ **do**
2: $\quad \bar{\boldsymbol{u}}_i = (\frac{M}{\Delta t} + K + A)^{-1}(\frac{M}{\Delta t}\bar{\boldsymbol{u}}_{i-1})$
3: **return** $\bar{\boldsymbol{u}}_N$

and approximate the operator $\widetilde{\mathcal{L}}$ by $\widetilde{\mathcal{L}}^d$ in the following way,

Algorithm 3 Discretize the operator $\widetilde{\mathcal{L}}$ as $\widetilde{\mathcal{L}}^d$

Input: $\bar{\boldsymbol{p}}_N$ and N
Output: $\bar{\boldsymbol{p}}_0$
1: **for** $i = N-1, N-2, \ldots, 0$ **do**
2: $\quad \bar{\boldsymbol{p}}_i = (\frac{M}{\Delta t} + K - A)^{-1}(\frac{M}{\Delta t}\bar{\boldsymbol{p}}_{i+1})$
3: **return** $\bar{\boldsymbol{p}}_0$

Therefore, the operator $\widetilde{\mathcal{L}}\mathcal{L} + \tau\mathrm{I}$ is discretized as $\widetilde{\mathcal{L}}^d\mathcal{L}^d + \tau\mathrm{I}_n$, which is actually a linear operator mapping from $\mathbb{R}^n$ to $\mathbb{R}^n$.

For the term $\min\left(\sigma_k\bar{u}_0 + \lambda^k + \beta, 0\right)$ of (3.15), the corresponding finite element approximation amounts to solve

$$\min_{\boldsymbol{v}\le 0}(\boldsymbol{v} - \boldsymbol{\omega}_h)^\top M(\boldsymbol{v} - \boldsymbol{\omega}_h), \quad \boldsymbol{v} \in \mathbb{R}^n, \tag{3.17}$$

where $\boldsymbol{\omega}_h \in \mathbb{R}^n$ is the finite element approximation of the function $\sigma_k\bar{u}_0 + \lambda^k + \beta$. Since the matrix M is not diagonal and high dimension of M leads to quite expensive computational cost when an iterative algorithm is applied, we replace M by its lumped mass matrix [31] given by

$$M = \mathrm{diag}(m_{ii}), \quad m_{ii} = \sum_{j=1}^{n}\int_\Omega \phi_i\phi_j dx.$$

We still denote the lumped matrix as M for convenience. More details about the discussions on the error analysis of the mass lumping technique applied to optimal control problems can be referred to [31, 36]. In this way, the finite element approximation of the term $\min\left(\sigma_k\bar{u}_0 + \lambda^k + \beta, 0\right)$ is

$$\min\left(\sigma_k\bar{\boldsymbol{u}}_0 + \boldsymbol{\lambda}^k + \beta\mathbf{1}, 0\right),$$

and the finite element approximation of the term $\max\left(\sigma_k\bar{u}_0^{k+1} + \lambda^k - \beta, 0\right)$ can be derived in the same way.

In summary, the discretized (3.15) can be written as

$$(\widetilde{\mathcal{L}}^d\mathcal{L}^d + \tau\mathrm{I})\bar{\boldsymbol{u}}_0 + \sigma_k\bar{\boldsymbol{u}}_0 - \min\left(\sigma_k\bar{\boldsymbol{u}}_0 + \boldsymbol{\lambda}^k + \beta\mathbf{1}, 0\right) - \max\left(\sigma_k\bar{\boldsymbol{u}}_0 + \boldsymbol{\lambda}^k - \beta\mathbf{1}, 0\right) = \widetilde{\mathcal{L}}^d(\boldsymbol{u}_T) - \boldsymbol{\lambda}^k. \tag{3.18}$$

Because the velocity v is assumed to be constant, we have $A^\top = -A$. Furthermore, there holds

$$\begin{aligned}\widetilde{\mathcal{L}}^d\mathcal{L}^d &= \left((\frac{M}{\Delta t}+K-A)^{-1}\frac{M}{\Delta t}\right)^N \cdot \left((\frac{M}{\Delta t}+K+A)^{-1}\frac{M}{\Delta t}\right)^N \\ &= \left((\frac{M}{\Delta t}+K+A)^{-\top}\frac{M}{\Delta t}\right)^N \cdot \left((\frac{M}{\Delta t}+K+A)^{-1}\frac{M}{\Delta t}\right)^N.\end{aligned}$$

Notice that the matrix $\widetilde{\mathcal{L}}^d\mathcal{L}^d$ is not symmetric, in order to obtain an equivalent equation with better structure, we multiple M in the both sides of (3.18), and finally obtain

$$\begin{aligned}&((\mathcal{L}^d)^\top \cdot M \cdot \mathcal{L}^d + \tau M)\bar{\boldsymbol{u}}_0 + \sigma_k M\bar{\boldsymbol{u}}_0 - M\min\left(\sigma_k\bar{\boldsymbol{u}}_0+\boldsymbol{\lambda}^k+\beta\mathbf{1},0\right) - M\max\left(\sigma_k\bar{\boldsymbol{u}}_0+\boldsymbol{\lambda}^k-\beta\mathbf{1},0\right)\\ &= M\widetilde{\mathcal{L}}^d(\boldsymbol{u}_T) - M\boldsymbol{\lambda}^k,\end{aligned} \tag{3.19}$$

where the left hand side term is from

$$\begin{aligned}M\widetilde{\mathcal{L}}^d\mathcal{L}^d &= M((\frac{M}{\tau}+K+A)^{-\top}\frac{M}{\tau})^N \cdot ((\frac{M}{\tau}+K+A)^{-1}\frac{M}{\tau})^N \\ &= (\frac{M}{\tau}(\frac{M}{\tau}+K+A)^{-\top})^N \cdot M \cdot ((\frac{M}{\tau}+K+A)^{-1}\frac{M}{\tau})^N \\ &= (\mathcal{L}^d)^\top \cdot M \cdot \mathcal{L}^d.\end{aligned} \tag{3.20}$$

For simplicity, let us define

$$\begin{aligned}G(\bar{\boldsymbol{u}}_0) :=&((\mathcal{L}^d)^\top \cdot M \cdot \mathcal{L}^d + \tau M)\bar{\boldsymbol{u}}_0 + \sigma_k M\bar{\boldsymbol{u}}_0 - M\min\left(\sigma_k\bar{\boldsymbol{u}}_0+\boldsymbol{\lambda}^k+\beta\mathbf{1},0\right)\\ &- M\max\left(\sigma_k\bar{\boldsymbol{u}}_0+\boldsymbol{\lambda}^k-\beta\mathbf{1},0\right),\end{aligned}$$

and finally, (3.19) can be represented as

$$G(\bar{\boldsymbol{u}}_0) = M\widetilde{\mathcal{L}}^d(\boldsymbol{u}_T) - M\boldsymbol{\lambda}^k. \tag{3.21}$$

We try to use the semi-smooth Newton (SSN) method to solve(3.21), which can expect to obtain a super-linear or even quadratic convergence rate.

Let $\bar{\boldsymbol{u}}_0^j$ denote results obtained by the j-th iteration of SSN. Then, define the active sets corresponding to $\bar{\boldsymbol{u}}_0^j$ by $\mathcal{A}_1^j := \{i \mid (\sigma_k\bar{\boldsymbol{u}}_0^j+\boldsymbol{\lambda}^k+\beta\mathbf{1},0)_i < 0\}$ and $\mathcal{A}_2^j := \{i \mid (\sigma_k\bar{\boldsymbol{u}}_0^j+\boldsymbol{\lambda}^k-\beta\mathbf{1},0)_i > 0\}$. Besides, let Π_1^j be a diagonal binary matrix with nonzero entries in $\mathcal{A}_1^j$ and Π_2^j be defined similarly corresponding to $\mathcal{A}_2^j$.

On this basis, the generalized Jacobian of $G(\cdot)$ (3.21) at $\bar{\boldsymbol{u}}_0^j$ is given by

$$G'(\bar{\boldsymbol{u}}_0^j) = (\mathcal{L}^d)^\top M\mathcal{L}^d + (\tau M + \sigma_k M(\mathrm{I}-\Pi_1^j-\Pi_2^j)). \tag{3.22}$$

Then, Newton system of the $(j+1)$-th iteration is

$$G(\bar{\boldsymbol{u}}_0^j) + G'(\bar{\boldsymbol{u}}_0^j)(\bar{\boldsymbol{u}}_0^{j+1}-\bar{\boldsymbol{u}}_0^j) = M\widetilde{\mathcal{L}}^d(\boldsymbol{u}_T) - M\boldsymbol{\lambda}^k. \tag{3.23}$$

It is simple to verify that $G'(\bar{\boldsymbol{u}}_0^j)$ is positive definite, hence the Newton system (3.23) admits a unique solution. Furthermore, since the matrix $G'(\bar{\boldsymbol{u}}_0^j)$ is positive definite, the conjugate gradient (CG) method can be applied to solving Newton system (3.23).

3.3 Preconditioned conjugate gradient method

Both the matrices $(\mathcal{L}^d)^\top M\mathcal{L}^d$ and $\mathcal{L}^d$ are extremely ill-conditioned, which leads to a deterioration of the convergence rate of CG method. To overcome these difficulties and accelerate each Newton iteration, it is necessary to add a novel and efficient pre-conditioner to the CG method.

Notice that the matrix $(\mathcal{L}^d)^\top M\mathcal{L}^d + \tau M$ is positive definite, it admits the following eigenvalue decomposition

$$(\mathcal{L}^d)^\top M\mathcal{L}^d + \tau M = \sum_{i=1}^{n} \lambda_i \boldsymbol{v}_i \boldsymbol{v}_i^\top, \tag{3.24}$$

with $\lambda_1 \geq \lambda_2 \geq \ldots \geq \lambda_n > 0$ and $\boldsymbol{v}_i$ be the eigenvector corresponding to λ_i. Let us choose the first $l+1$ largest eigenvalues and approximate the matrix $(\mathcal{L}^d)^\top M\mathcal{L}^d + \tau M$ as follows:

$$(\mathcal{L}^d)^\top M\mathcal{L}^d + \tau M \approx \mathcal{V} := \sum_{i=1}^{l} \lambda_i \boldsymbol{v}_i \boldsymbol{v}_i^\top + \lambda_{l+1} \sum_{i=l+1}^{n} \boldsymbol{v}_i \boldsymbol{v}_i^\top, \tag{3.25}$$

and then $G'(\bar{\boldsymbol{u}}_0^j)$ defined in (3.22) can be approximated by $\mathcal{G}$,

$$\mathcal{G} := \mathcal{V} + \sigma_k M(\mathrm{I} - \Pi_1^j - \Pi_2^j). \tag{3.26}$$

Thus, we choose $\mathcal{G}$ as the pre-conditioner for $G'(\bar{\boldsymbol{u}}_0^j)$.

Define

$$W := \lambda_{l+1}\mathrm{I} + \sigma_k M(\mathrm{I} - \Pi_1^j - \Pi_2^j), \quad V := [\boldsymbol{v}_1, \boldsymbol{v}_2, \ldots, \boldsymbol{v}_l],$$
$$C := \mathrm{diag}(\lambda_1 - \lambda_{l+1}, \lambda_2 - \lambda_{l+1}, \ldots, \lambda_l - \lambda_{l+1}).$$

Then, there holds

$$\mathcal{G}^{-1} = W^{-1} - W^{-1}V(C^{-1} + V^\top W^{-1}V)^{-1}V^\top W^{-1}. \tag{3.27}$$

Notice that W is a diagonal matrix which means W^{-1} can be obtained easily and the matrix $(C^{-1} + V^\top W^{-1}V)^{-1}$ is an small-scale, namely, l by l matrix. Hence, for any vector $\boldsymbol{x} \in \mathbb{R}^n$ the computational cost of $\mathcal{G}^{-1}\boldsymbol{x}$ is cheap.

Then, the spectral property of $\mathcal{G}^{-1}G'(\bar{\boldsymbol{u}}_0^j)$ is analyzed as follows:

Theorem 3.3. *Let ξ be an eigenvalue of the matrix $\mathcal{G}^{-1}G'(\bar{\boldsymbol{u}}_0^j)$, $\lambda_1 \geq \lambda_2 \geq \ldots \geq \lambda_n$ be the n eigenvalues of $(\mathcal{L}^d)^\top M\mathcal{L}^d + \tau M$. Then, we have $\frac{\lambda_n}{\lambda_{l+1}} \leq \xi \leq 1$.*

Proof. The upper bound $\xi \leq 1$ holds because there holds

$$\mathcal{G} - G'(\bar{\boldsymbol{u}}_0^j) = \sum_{i=l+1}^{n} (\lambda_{l+1} - \lambda_i)\boldsymbol{v}_i \boldsymbol{v}_i^\top \succeq 0.$$

Let ξ be an eigenvalue of $\mathcal{G}^{-1}G'(\bar{\boldsymbol{u}}_0^j)$ and $\boldsymbol{y}$ be an eigenvector corresponding to the eigenvalue ξ, then we have

$$\xi = \frac{\boldsymbol{y}^\top G'(\bar{\boldsymbol{u}}_0^j)\boldsymbol{y}}{\boldsymbol{y}^\top \mathcal{G}\boldsymbol{y}} \geq \frac{\boldsymbol{y}^\top((\mathcal{L}^d)^\top M\mathcal{L}^d + \tau M)\boldsymbol{y}}{\boldsymbol{y}^\top \mathcal{V}\boldsymbol{y}} \geq \lambda_{\min}(((\mathcal{L}^d)^\top M\mathcal{L}^d + \tau M)\mathcal{V}^{-1}),$$

where $\lambda_{\min}(\cdot)$ denotes the minimal eigenvalue of a matrix. The first inequality holds from (3.22), (3.26) and the fact that the matrix $\tau M + \sigma_k M(\mathrm{I} - \Pi_1^j - \Pi_2^j)$ is positive definite. By (3.24) and (3.25), the lower bound is obtained directly. □

Remark 3.4. For the implementation of the proposed PCG method, we need to obtain the $l+1$ largest eigenvalues and the corresponding eigenvectors. This procedure can be done efficiently by Lanczos method [32,34].

Finally, the sub-problem (3.6) can be solved by the following SSN-PCG algorithm.

Algorithm 4 SSN-PCG method

Step 0: Given l, using Lanczos method to obtain the first $l+1$ largest eigenvalues and corresponding eigenvectors, $\bar{\boldsymbol{u}}_0^0$, tolerance $tol > 0$. Set $j = 0$.

Step 1: Construct the Newton system (3.23) and solve it by PCG method with the pre-conditioner chosen by $\mathcal{G}$ (3.26), where $\mathcal{G}^{-1}$ is given by (3.27).

Step 2: Compute $\|G(\bar{\boldsymbol{u}}_0^{j+1}) - M\widetilde{\mathcal{L}}^d(\boldsymbol{u}_T) + M\boldsymbol{\lambda}^k\|$, where $\bar{\boldsymbol{u}}_0^{j+1}$ is the solution of (3.23) at the $(j+1)$-th iterate. If

$$\|G(\bar{\boldsymbol{u}}_0^{j+1}) - M\widetilde{\mathcal{L}}^d(\boldsymbol{u}_T) + M\boldsymbol{\lambda}^k\| \le tol,$$

we take $\bar{\boldsymbol{u}}_0^{j+1}$ as the solution and terminate the iteration; otherwise set $j = j+1$ and return to **Step 2**.

In summary, the whole process of solving Problem $(\tilde{P})$ can be explained below,

Algorithm 5 ALM-SSN-PCG method

Step 1: Let σ_0 be a given parameter, $\{\epsilon_k\}$ be a summable sequence of non-negative numbers, and initialize $\boldsymbol{\lambda}^0 \in \mathbb{R}^n$. Set $k = 0$.

Step 2: Solve problem (3.21) with $tol := \epsilon_k$ by Algorithm 4 to obtain $\bar{\boldsymbol{u}}_0^{k+1}$ and

$$\bar{\boldsymbol{z}}^{k+1} = \min\left(\bar{\boldsymbol{u}}_0^{k+1} + \frac{\boldsymbol{\lambda}^k + \beta\mathbf{1}}{\sigma_k}, 0\right) + \max\left(\bar{\boldsymbol{u}}_0^{k+1} + \frac{\boldsymbol{\lambda}^k - \beta\mathbf{1}}{\sigma_k}, 0\right).$$

Step 3: Compute

$$\boldsymbol{\lambda}^{k+1} = \boldsymbol{\lambda}^k + \sigma_k(\bar{\boldsymbol{u}}_0^{k+1} - \boldsymbol{z}^{k+1}), \tag{3.28}$$

and update the parameter $\sigma_k \le \sigma_{k+1} \uparrow \sigma_\infty \le +\infty$. Set $k = k+1$ and return to **Step 2.**

4 Numerical solution procedure of second stage

Let u_0^* denote the results obtained by the ALM-SSN-PCG method. It may not satisfy the desired sparsity property (1.2). Thus, we introduce a post-processing procedure in the second stage to enhance the sparsity structure of the obtained solution and find the intensities of the initial sources.

We first compute all local maxima $\{x_i\}_{i=1}^m$ of $\mid u_0^* \mid$ whose values is close to optimal locations [4,24]. $m \in \mathbb{N}$ represents the number of local maxima of $\mid u_0^* \mid$. The initial source $\hat{u}_0^*$ is thus expressed as

$$\hat{u}_0^* := \sum_{i=1}^m \alpha_i \delta_{x_i},$$

and the final state $\mathcal{L}(\hat{u}_0^*)$ is given by

$$\mathcal{L}(\hat{u}_0^*) = \sum_{i=1}^m \mathcal{L}(\delta_{x_i})\alpha_i.$$

Then, we aim to find the optimal intensities $\{\alpha_i\}_{i=1}^m$ such that the obtained final state $\mathcal{L}(\hat{u}_0^*)$ is close enough to the observation u_T, namely,

$$\min_{\{\alpha_i\}_{i=1}^m} \quad \|\sum_{i=1}^m \mathcal{L}(\delta_{x_i})\alpha_i - u_T\|^2. \tag{4.1}$$

Applying the space and time discretization as discussed in Sub-section 3.2, problem (4.1) is discretized as a least-square fitting problem,

$$\min_{\boldsymbol{\alpha}} \quad \|L\alpha - \boldsymbol{u}_T\|^2, \tag{4.2}$$

where $\boldsymbol{\alpha} := \{\alpha_i\}_{i=1}^l$, $L \in \mathbb{R}^{n\times l}$ with j-th column be the finite element approximation of $\mathcal{L}(\delta_{x_j})$ and $\boldsymbol{u}_T$ be the finite element approximation of the function u_T. It is worth noting that (4.2) is equivalent to solve

$$L^\top L\boldsymbol{\alpha} = L^\top \boldsymbol{u}_T, \tag{4.3}$$

We summarize the whole process of solving the identification problem as follows.

Algorithm 6 Two-stage numerical method

Stage 1: Construct the optimal control problem (P) and obtain the corresponding solution u_0^* by Algorithm 5.

Stage 2:

Step 2.1: Compute all local maxima $\{x_i\}_{i=1}^m$ of $\mid u_0^* \mid$;

Step 2.2: Compute the matrix L whose j-th column is the finite element approximation of $\mathcal{L}(\delta_{x_j})$ and the finite element approximation $\boldsymbol{u}_T$ of the function u_T. Then the intensities $\{\alpha_i\}_{i=1}^m$ are obtained by solving the following equation:

$$L^\top L\boldsymbol{\alpha} = L^\top \boldsymbol{u}_T.$$

Output: Numerical solution $\hat{u}_0^*$ is given by

$$\hat{u}_0^* = \sum_{i=1}^m \alpha_i \delta_{x_i}.$$

5 Convergence Analysis

In this section, we will analyze the convergence property and estimate the super-linear convergence rate in the non-ergodic sense for using inexact ALM method to solve Problem $(\tilde{P})$. It is worth noting that Problem $(\tilde{P})$ is formulated in an infinite dimensional space and an inexactness criterion (3.4) is incorporated into inexact ALM method, hence the existing theoretical results developed in the finite dimensional space [13, 26, 30] are not applicable.

5.1 Global Convergence

Firstly, from (3.4) there holds

$$e^{k+1} \in \partial L_{\sigma_k}(u_0^{k+1}, z^{k+1}; \lambda^k) = \begin{pmatrix} Df(u_0^{k+1}) + \lambda^k + \sigma_k(u_0^{k+1} - z^{k+1}) \\ \partial g(z^{k+1}) - \lambda^k - \sigma_k(u_0^{k+1} - z^{k+1}) \end{pmatrix}, \tag{5.1}$$

where $Df(u_0^{k+1})$ denotes the first-order differential of the functional $f(\cdot)$ at u_0^{k+1}. Let us define $e^{k+1} = (e_{u_0}^{k+1}, e_z^{k+1})^\top$ and combine with (3.5), the equations (3.4)-(3.5) can be rewritten as follows:

$$Df(u_0^{k+1}) + \lambda^{k+1} = e_{u_0}^{k+1}, \tag{5.2}$$

$$g(z) - g(z^{k+1}) \geq \langle \lambda^{k+1} + e_z^{k+1}, z - z^{k+1} \rangle, \tag{5.3}$$

$$\lambda^{k+1} = \lambda^k + \sigma_k(u_0^{k+1} - z^{k+1}). \tag{5.4}$$

To proceed the further analysis, we introduce the following notations

$$\omega = \begin{pmatrix} u_0 \\ z \\ \lambda \end{pmatrix}, \quad F(\omega) = \begin{pmatrix} Df(u_0) + \lambda \\ -\lambda \\ -u_0 + z \end{pmatrix}. \tag{5.5}$$

The optimal solution of Problem $(\tilde{P})$ denoted as ω^* satisfies

$$g(z) - g(z^*) + \langle F(\omega^*), \omega - \omega^* \rangle \geq 0, \quad \forall \omega \in L^2(\Omega) \times L^2(\Omega) \times L^2(\Omega). \tag{5.6}$$

The following lemma characterizes the difference between the iteration point ω^{k+1} and the solution ω^* according to the optimality condition (5.6).

Lemma 5.1. *Let $\omega^{k+1} = (u_0^{k+1}, z^{k+1}, \lambda^{k+1})^\top$ be the $(k+1)$-th iteration points. Then, there holds*

$$g(z) - g(z^{k+1}) + \langle F(\omega^{k+1}), \omega - \omega^{k+1} \rangle \geq \left\langle \begin{pmatrix} e_{u_0}^{k+1} \\ e_z^{k+1} \\ \frac{\lambda^k - \lambda^{k+1}}{\sigma_k} \end{pmatrix}, \omega - \omega^{k+1} \right\rangle, \quad \forall \omega \in L^2(\Omega) \times L^2(\Omega) \times L^2(\Omega). \tag{5.7}$$

Proof. The conclusion holds from (5.2), (5.3) and (5.4) directly. □

The following lemma plays an important role on our convergence analysis.

Lemma 5.2. *Let the sequence $\{\omega^k\}$ be generated by Algorithm 1 and the solution be $\omega^* := (u_0^*, z^*, \lambda^*)^\top$, respectively. There holds that*

$$\frac{\tau}{2}\|u_0^{k+1} - u_0^*\|^2 + \frac{\|\lambda^k - \lambda^{k+1}\|^2}{4\sigma_k} + \frac{\|\lambda^{k+1} - \lambda^*\|^2}{2\sigma_{k+1}} \leq \frac{\|\lambda^k - \lambda^*\|^2}{2\sigma_k} + \frac{\|e^k\|^2}{\tau} + \frac{\|e_z^{k+1}\|^2}{\sigma_k}. \tag{5.8}$$

Proof. Setting the arbitrary ω in (5.7) as the solution ω^*, there holds

$$\begin{aligned} & \langle e_{u_0}^{k+1}, u_0^{k+1} - u_0^* \rangle + \langle e_z^{k+1}, z^{k+1} - z^* \rangle + \frac{\langle \lambda^k - \lambda^{k+1}, \lambda^{k+1} - \lambda^* \rangle}{\sigma_k} \\ \geq\ & g(z^{k+1}) - g(z^*) + \langle F(\omega^{k+1}), \omega^{k+1} - \omega^* \rangle. \end{aligned} \tag{5.9}$$

For the right hand side term, we have

$$\begin{aligned} & g(z^{k+1}) - g(z^*) + \langle F(\omega^{k+1}), \omega^{k+1} - \omega^* \rangle \\ =\ & g(z^{k+1}) - g(z^*) + \langle F(\omega^*), \omega^{k+1} - \omega^* \rangle + \langle F(\omega^{k+1}) - F(\omega^*), \omega^{k+1} - \omega^* \rangle \\ \geq\ & \langle Df(u_0^{k+1}) - Df(u_0^*), u_0^{k+1} - u_0^* \rangle. \end{aligned} \tag{5.10}$$

The last equality is from the variational inequality (5.6) and the definition of $F(\cdot)$ (5.5). Because the definition of the functional $f(\cdot)$ (3.2), which implies the strictly convexity, we have

$$\langle Df(u_0^{k+1}) - Df(u_0^*), u_0^{k+1} - u_0^* \rangle \geq \tau \|u_0^{k+1} - u_0^*\|^2. \tag{5.11}$$

For the term $\langle \lambda^k - \lambda^{k+1}, \lambda^{k+1} - \lambda^* \rangle$, there holds

$$\langle \lambda^k - \lambda^{k+1}, \lambda^{k+1} - \lambda^* \rangle = \frac{\|\lambda^k - \lambda^*\|^2 - \|\lambda^{k+1} - \lambda^*\|^2 - \|\lambda^k - \lambda^{k+1}\|^2}{2}. \tag{5.12}$$

Combining (5.9), (5.10), (5.11) and (5.12), we obtain that

$$\langle e_{u_0}^{k+1}, u_0^{k+1} - u_0^* \rangle + \langle e_z^{k+1}, z^{k+1} - z^* \rangle + \frac{\|\lambda^k - \lambda^*\|^2}{2\sigma_k} \geq \frac{\|\lambda^{k+1} - \lambda^*\|^2}{2\sigma_k} + \frac{\|\lambda^k - \lambda^{k+1}\|^2}{2\sigma_k} + \tau \|u_0^{k+1} - u_0^*\|^2. \quad (5.13)$$

Next, we shall approximate the first two terms of (5.13).

$$\begin{aligned} & \langle e_{u_0}^{k+1}, u_0^{k+1} - u_0^* \rangle + \langle e_z^{k+1}, z^{k+1} - z^* \rangle \\ = \; & \langle e_{u_0}^{k+1} + e_z^{k+1}, u_0^{k+1} - u_0^* \rangle - \langle e_z^{k+1}, u_0^{k+1} - z^{k+1} \rangle \\ = \; & \langle e_{u_0}^{k+1} + e_z^{k+1}, u_0^{k+1} - u_0^* \rangle - \left\langle e_z^{k+1}, \frac{\lambda^{k+1} - \lambda^k}{\sigma_k} \right\rangle \\ \leq \; & \frac{\tau}{2} \|u_0^{k+1} - u_0^*\|^2 + \frac{\|\lambda^k - \lambda^{k+1}\|^2}{4\sigma_k} + \frac{\|e_{u_0}^{k+1} + e_z^{k+1}\|^2}{2\tau} + \frac{\|e_z^{k+1}\|^2}{\sigma_k} \\ \leq \; & \frac{\tau}{2} \|u_0^{k+1} - u_0^*\|^2 + \frac{\|\lambda^k - \lambda^{k+1}\|^2}{4\sigma_k} + \frac{\|e^k\|^2}{\tau} + \frac{\|e_z^{k+1}\|^2}{\sigma_k}. \end{aligned} \quad (5.14)$$

Combining (5.13) with (5.14), we obtain

$$\frac{\|e^k\|^2}{\tau} + \frac{\|e_z^{k+1}\|^2}{\sigma_k} + \frac{\|\lambda^k - \lambda^*\|^2}{2\sigma_k} \geq \frac{\|\lambda^{k+1} - \lambda^*\|^2}{2\sigma_k} + \frac{\|\lambda^k - \lambda^{k+1}\|^2}{4\sigma_k} + \frac{\tau}{2} \|u_0^{k+1} - u_0^*\|^2. \quad (5.15)$$

Because of (5.15) and the increasing parameter sequence $\{\sigma_k\}$, the conclusion holds. □

Then, we can prove the global convergence of the inexact ALM method.

Theorem 5.3. *Let the sequence $\{\omega^k\}$ be generated by Algorithm 1 and the solution be $\omega^* := (u_0^*, z^*, \lambda^*)^\top$, respectively. Then, $\{\omega^k\}$ converges to ω^* strongly in L^2 space.*

Proof. Let us sum (5.8) over $k = 0, 1, \ldots, \infty$, there holds

$$\begin{aligned} & \sum_{k=0}^{\infty} \left(\frac{\tau}{2} \|u_0^{k+1} - u_0^*\|^2 + \frac{\|\lambda^k - \lambda^{k+1}\|^2}{4\sigma_k} \right) \\ \leq \; & \frac{\|\lambda^0 - \lambda^*\|^2}{2\sigma_0} + \sum_{k=0}^{\infty} \left(\frac{\|e^k\|^2}{\tau} + \frac{\|e_z^{k+1}\|^2}{\sigma_k} \right) \\ \leq \; & \frac{\|\lambda^0 - \lambda^*\|^2}{2\sigma_0} + \left(\frac{1}{\tau} + \frac{1}{\sigma_0} \right) \sum_{k=0}^{\infty} \epsilon_k^2. \end{aligned} \quad (5.16)$$

Because $\{\epsilon_k\}$ is a summable sequence, we have $\sum_{k=0}^{\infty} \epsilon_k^2 < \infty$, this means the term

$$\sum_{k=0}^{\infty} \left(\frac{\tau}{2} \|u_0^{k+1} - u_0^*\|^2 + \frac{\|\lambda^k - \lambda^{k+1}\|^2}{4\sigma_k} \right)$$

is convergent, hence we can further obtain that

$$\|u_0^{k+1} - u_0^*\| \to 0, \quad \text{and} \quad \frac{\|\lambda^k - \lambda^{k+1}\|^2}{\sigma_k} \to 0, \quad \text{as} \quad k \to \infty, \quad (5.17)$$

which means $\{u_0^k\}$ converges to u_0^* strongly in L^2 space.

Because there holds

$$\frac{\|\lambda^k - \lambda^{k+1}\|^2}{\sigma_k} = \sigma_k \|u_0^{k+1} - z^{k+1}\|,$$

combining with the increasing non-negative parameter sequence $\{\sigma_k\}$, we have $\|u_0^{k+1} - z^{k+1}\| \to 0$ as $k \to \infty$. Besides, we have

$$\|z^{k+1} - z^*\| \leq \|z^{k+1} - u_0^{k+1}\| + \|u_0^{k+1} - u^*\|,$$

which implies that $\{z^k\}$ converges to z^* strongly in L^2 space.

Furthermore, from (5.2) and combining with $\|e_{u_0}^{k+1}\| \to 0$ and $u_0^{k+1} \to u_0^*$ as $k \to \infty$, the sequence $\{\lambda^k\}$ strongly converges to $-DJ(u_0^*)$ in L^2 space. From the variational inequality (5.6), we have $\lambda^* = -DJ(u_0^*)$, and thus $\{\lambda^k\}$ converges to λ^* strongly in L^2 space. The proof is then complete. □

5.2 Convergence Rate

In this sub-section, we estimate the convergence rate of the inexact ALM method in the non-ergodic sense [25].

To proceed further estimation, let us define the functional $G(\cdot)$ by

$$G(e_{u_0}, e_z, u, z) := \|e_{u_0}\|^2 + \|e_z\|^2 + \|u - z\|^2. \tag{5.18}$$

It follows from (5.6) and (5.7) that the current iterate $\omega^k = (u_0^k, z^k, \lambda^k)^\top$ is the optimal solution if and only if $G(e_{u_0}^k, e_z^k, u^k, z^k) = 0$.

Theorem 5.4. *Suppose that the sequence $\{\omega^k\}$ generated by Algorithm 1 converges to the solution $\omega^* := (u_0^*, z^*, \lambda^*)^\top$. Then, for any $k \in \mathbb{N}$, we have*

(a). For the case that the penalty parameter $\sigma_k \uparrow \sigma_\infty = \infty$, there holds

$$G(e_{u_0}^{k+1}, e_z^{k+1}, u^{k+1}, z^{k+1}) \leq \epsilon_{k+1}^2 + o\left(\frac{1}{\sigma_k}\right). \tag{5.19}$$

(b). For the case that the penalty parameter $\sigma_k \uparrow \sigma_\infty < \infty$, there holds

$$\min_{0 \leq i \leq k} G(e_{u_0}^{i+1}, e_z^{i+1}, u^{i+1}, z^{i+1}) = o\left(\frac{1}{k}\right). \tag{5.20}$$

Proof. (a). It follows from (5.8) that

$$\begin{aligned} &\frac{1}{4}\sigma_k \|u^{k+1} - z^{k+1}\|^2 = \frac{\|\lambda^k - \lambda^{k+1}\|^2}{4\sigma_k} \\ \leq\ & \left(\frac{\|\lambda^k - \lambda^*\|^2}{2\sigma_k} - \frac{\|\lambda^{k+1} - \lambda^*\|^2}{2\sigma_{k+1}}\right) + \left(\frac{\|e^k\|^2}{\tau} + \frac{\|e_z^{k+1}\|^2}{\sigma_k}\right) \\ \leq\ & \left(\frac{\|\lambda^k - \lambda^*\|^2}{2\sigma_k} - \frac{\|\lambda^{k+1} - \lambda^*\|^2}{2\sigma_{k+1}}\right) + \left(\frac{1}{\tau} + \frac{1}{\sigma_k}\right)\epsilon_k^2. \end{aligned} \tag{5.21}$$

Because $\{\lambda^k\}$ converges to λ^* strongly in L^2 space and $\{\epsilon_k\}$ is a summable and non-negative sequence, there holds

$$\left(\frac{\|\lambda^k - \lambda^*\|^2}{2\sigma_k} - \frac{\|\lambda^{k+1} - \lambda^*\|^2}{2\sigma_{k+1}}\right) + \left(\frac{1}{\tau} + \frac{1}{\sigma_k}\right)\epsilon_k^2 \to 0.$$

Combining with (5.21), we conclude that $\|u^{k+1} - z^{k+1}\|^2 = o(1/\sigma_k)$. Combining with the definition of $\{e^k\}$ and $\|e^k\| \leq \epsilon_k$, the conclusion holds.

(b). From (5.21), we obtain

$$\sum_{k=0}^{\infty}(\sigma_k\|u^{k+1} - z^{k+1}\|^2 + \|e^k\|^2) \leq \frac{2\|\lambda^0 - \lambda^*\|^2}{\sigma_0} + \left(\frac{4}{\tau} + \frac{4}{\sigma_0} + 1\right)\sum_{k=0}^{\infty}\epsilon_k^2. \tag{5.22}$$

Due to the summable and non-negative sequence $\{\epsilon_k\}$, the right hand side term converges to some constant a, which is defined as

$$a := \frac{2\|\lambda^0 - \lambda^*\|^2}{\sigma_0} + \left(\frac{4}{\tau} + \frac{4}{\sigma_0} + 1\right)\sum_{k=0}^{\infty}\epsilon_k^2.$$

From (5.22), there holds

$$\sum_{k=0}^{\infty}\min_{0\leq i\leq k}\{\sigma_i\|u^{i+1} - z^{i+1}\|^2 + \|e^i\|^2\} \leq \sum_{k=0}^{\infty}(\sigma_k\|u^{k+1} - z^{k+1}\|^2 + \|e^k\|^2) \leq a.$$

Notice that the sequence $\{\min_{0\leq i\leq k}\{\sigma_i\|u^{i+1} - z^{i+1}\|^2 + \|e^i\|^2\}\}$ is monotonically decreasing, which further implies that

$$\min_{0\leq i\leq k}\{\sigma_i\|u^{i+1} - z^{i+1}\|^2 + \|e^i\|^2\} = o\left(\frac{1}{k}\right) \quad \text{as} \quad k \to \infty.$$

Due to the increasing sequence $\{\sigma_k\}$, we have

$$\min_{0\leq i\leq k}\{\sigma_i\|u^{i+1} - z^{i+1}\|^2 + \|e^i\|^2\} \geq \min(\sigma_0, 1)\min_{0\leq i\leq k}\{\|u^{i+1} - z^{i+1}\|^2 + \|e^i\|^2\},$$

and thus there holds

$$\min_{0\leq i\leq k}\{\|u^{i+1} - z^{i+1}\|^2 + \|e^i\|^2\} = o\left(\frac{1}{k}\right) \quad \text{as} \quad k \to \infty.$$

Then, we complete the proof. □

Remark 5.5. It is worth noting that the convergence rate of the inexact ALM method depends on the choice of the penalty parameter sequence $\{\sigma_k\}$ and the inexactness parameter $\{\epsilon_k\}$. More specifically, a too small sequence $\{\sigma_k\}$ can results in an $o(1/k)$ worst-case convergence rate which is not ideal in practice. Furthermore, from the statement (a) of Theorem 5.4, the worst-case convergence rate can be even super-linear if we choose the sequence $\{\sigma_k = \theta^k\}$ and $\{\epsilon_k = o(1/\theta^k)\}$ with $\theta > 1$.

6 Numerical experiment

To show the efficiency and accuracy of proposed two-stage numerical method, we apply the proposed method to solve three different types of initial source identification problems in this section. Firstly, we set the time step $\Delta t = 0.02$ and the mesh size $\Delta x = 0.02$ to discretize the problem. The regularization parameters are chosen as $\tau = 10^{-5}$ and $\beta = \Delta x^4$, as done in [4, 24]. Then, we use the designed two-stage method to solve the problem.

In the first stage, the stopping criterion for ALM-SSN-PCG method (Algorithm 5) is given by

$$\|u_0^k - z^k\| \leq 10^{-6}.$$

The penalty parameter sequence is chosen as $\sigma_k = 5^k$ and the initial guess $\boldsymbol{\lambda}^0 = 0$. For the SSN-PCG method, we set $tol = \epsilon_k = \min(\frac{10^{-3-k}}{k}, 10^{-6})$. Additionally, setting $l = 100$ for constructing the pre-conditioner of the Newton system, more clearly, we choose the first 100 largest eigenvalues and the corresponding eigenvectors of $(\mathcal{L}^d)^\top M\mathcal{L}^d + \tau M$. The Lanczos method proceeded in the pre-conditioner construction is done by the default MATLAB solver 'eigs' and the Newton system is solved by the default MATLAB solver 'pcg' with the tolerance 10^{-6}.

For comparison, ALM-SSN-CG method which is the proposed Algorithm 6 without using preconditioning technique to solve Newton system, primal dual hybrid gradient (PDHG) method [4] and gradient descend (GD) method [24] are also applied to solve examples. Furthermore, to show the robustness of proposed method, $u_T(x)$ is constructed by adding a function $\delta \in L^2(\Omega)$ and satisfying $\|\delta\|_{L^2(\Omega)} = 0.1\|\mathcal{L}(u_0^*)\|_{L^2(\Omega)}$ with a given function u_0^*.

All numerical experiments are done in MATLAB 2019b and conducted on a computer with Inter(R) Core(TM) i7-7660U CPU at 2.50GHz and 32GB RAM.

6.1 Example 1: initial source identification problem defined in homogeneous medium

Consider the linear diffusion-advection equation (1.1) modeled in a homogeneous medium, where the diffusivity coefficient $d = 0.05$, the advection vector $v = (2, -2)^\top$, the space domain $\Omega = (0, 2) \times (0, 1)$ and the terminal time $T = 0.1$.

The L^2 regularization parameter τ is set to be $\tau = 10^{-i}$ with $i = 5, 4, 3, 2$ and apply four different methods to solving such problem. All the results are listed in Table 1. 'Iter' represents the iteration number. In both PDHG and GD method, we provide the total iteration number, and in other methods, the total iteration number of ALM/SSN/PCG (ALM/SSN/CG) method is listed in order. 'CPU' denotes running time of each algorithm. Besides, We also indicate in the table whether the algorithm converges. From Table 1, we notice that our proposed algorithm is much more efficient than PDHG method and GD method especially when τ is extremely small. Furthermore, our proposed algorithm converges fast for all cases, while the convergence performance of PDHG method is very slow for $\tau = 10^{-3}, 10^{-4}, 10^{-5}$ and GD method does not converge for all cases even when the maximal iteration number is achieved. This validates the convergence rate of our proposed algorithm is superior to that of PDHG method and GD method. Besides, we also compare the proposed method with ALM-SSN-CG method to illustrate the effectiveness of the designed pre-conditioner. The number of internal iteration of the proposed method is always much less than that of ALM-SSN-CG method, which demonstrates that our designed preconditioner can improve the spectral property of each Newton system and thus accelerate the convergence rate of CG method efficiently. It is worth noting that the SSN method can achieve local super-linear convergence rate only when each Newton system is solved to a high accuracy. The pre-conditioner can not only improve the convergence rate of CG method but also help CG method obtain a more accurate solution.

Table 1: Numerical results obtained by four methods with different τ for Example 1.

τ	Method	Iter	Convergence	CPU(sec)
10^{-5}	ALM-SSN-PCG	2/4/106	Yes	2.32
	ALM-SSN-CG	2/11/924	Yes	12.31
	PDHG	5000	No	60.88
	GD	5000	No	61.42
10^{-4}	ALM-SSN-PCG	2/4/50	Yes	1.16
	ALM-SSN-CG	2/6/498	Yes	5.59
	PDHG	3446	Yes	43.06
	GD	5000	No	62.12
10^{-3}	ALM-SSN-PCG	2/4/19	Yes	0.55
	ALM-SSN-CG	2/4/280	Yes	3.14
	PDHG	499	Yes	6.23
	GD	5000	No	61.34
10^{-2}	ALM-SSN-PCG	2/4/11	Yes	0.37
	ALM-SSN-CG	2/4/122	Yes	1.49
	PDHG	69	Yes	0.88
	GD	5000	No	63.17

Then, we test our proposed algorithm for different mesh sizes and list the numerical results in Table 2. '#ALM', '#SSN' and '#PCG (#CG)' respectively denote the total iteration number of the corresponding methods. From Table 2, we notice that the convergence performance of the ALM method does not be affected by the mesh size of the discretization. Although the discretized ALM sub-problem (3.6) is of larger scale and more ill-conditioning when the mesh size is finer, the total iteration numbers of both SSN method and PCG method do not increase greatly, which means the designed algorithm and pre-conditioner is efficient and robust to mesh sizes. Thus, the convergence behavior of the new approach can be mesh independent in practice. Furthermore, we notice that our method behaves more efficient than ALM-SSN-CG method in term of 'CPU'.

Table 2: Comparison of our method with ALM-SSN-CG method with different mesh sizes for Example 1.

$(\Delta t, \Delta x)$	Method	#ALM	#SSN	#PCG(#CG)	CPU(sec)
$(\frac{1}{20}, \frac{1}{40})$	ALM-SSN-PCG	3	6	417	3.77
	ALM-SSN-CG	3	30	2698	6.73
$(\frac{1}{40}, \frac{1}{80})$	ALM-SSN-PCG	2	4	118	7.31
	ALM-SSN-CG	2	8	655	25.51
$(\frac{1}{60}, \frac{1}{120})$	ALM-SSN-PCG	1	2	24	6.97
	ALM-SSN-CG	1	3	199	41.33
$(\frac{1}{80}, \frac{1}{160})$	ALM-SSN-PCG	1	2	21	17.52
	ALM-SSN-CG	1	3	194	127.35

Finally, employing the new method, we successfully restore the initial state and illustrate the resulting solution $\hat{u}_0^*$ alongside the corresponding final state in Figure 1. Notably, the initial source is accurately recovered. Moreover, we evaluate the impact of noisy observation u_T by comparing numerical solutions obtained via two approaches: solving Problem (P) with L^2 regularization parameter $\tau = 10^{-5}$ and solving it with $\tau = 0$, as proposed in [24]. The comparative results are presented in Figure 2. It is evident that the solution derived from Problem (P) with $\tau = 10^{-5}$ effectively reconstructs both the locations and intensities of the initial source. Conversely, the solution from Problem (P) with $\tau = 0$ fails to accurately recover either the locations or the intensities. This discrepancy arises from the significantly higher ill-conditioning of Problem (P) with $\tau = 0$ compared to that with $\tau > 0$, rendering the solution more sensitive to the input data.

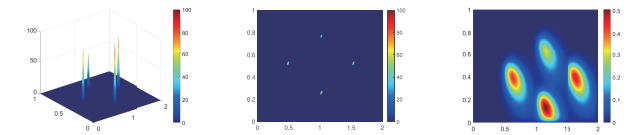

(a) Reference initial state (front view) (b) Reference initial state (above view) (c) Target u_T

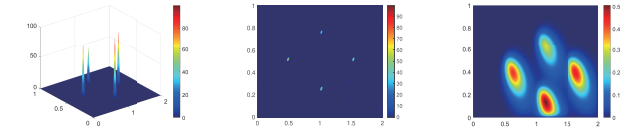

(d) Recovered initial state (front view) (e) Recovered initial state (above view) (f) Recovered final state

Figure 1: Source identification using new method for Example 1 with exact observation u_T.

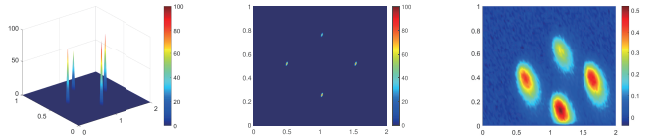

(a) Reference initial state (front view) (b) Reference initial state (above view) (c) Target u_T with noisy observation

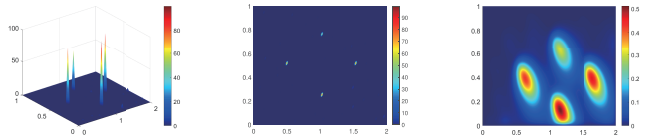

(d) Recovered initial state (front view) (e) Recovered initial state (above view) (f) Recovered final state

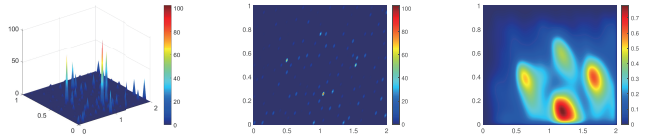

(g) Recovered initial state (front view) (h) Recovered initial state (above view) (i) Recovered final state

Figure 2: Source identification using new method for Example 1 with noisy observation u_T.

6.2 Example 2: initial source identification problem defined in heterogeneous medium

The linear diffusion-advection equation (1.1) is modeled in a heterogeneous medium. The space domain $\Omega = (0, 2) \times (0, 1)$ and the terminal time $T = 0.1$. The diffusivity coefficient $d = 0.08$ on $(0, 1) \times (0, 1)$ and $d = 0.05$ on $(1, 2) \times (0, 1)$, and the advection vector $v = (1, 2)^\top$.

We first set $\tau = 10^{-i}$ with $i = 5, 4, 3, 2$ and apply four methods to solving the reformulated optimal control problem (P). The detailed numerical results are reported in Table 3. It can be observed that the ALM sub-problem generated by the new method tends to be much more ill-conditioning when the regularization parameter τ becomes smaller. However,

the total iteration number of PCG method does not increase greatly for the extremely small τ, which means the pre-conditioner is robust to the regularization parameter τ. Due to the local super-linear convergence rate of the SSN method and the efficiency of the designed PCG method, the total computational cost of the proposed method is cheap.

Table 3: Numerical results obtained by four methods with different τ for Example 2.

τ	Method	Iter	Convergence	CPU(sec)
10^{-5}	ALM-SSN-PCG	2/4/85	Yes	1.77
	ALM-SSN-CG	2/10/879	Yes	9.87
	PDHG	5000	No	60.28
	GD	5000	No	60.57
10^{-4}	ALM-SSN-PCG	2/4/36	Yes	0.85
	ALM-SSN-CG	2/6/494	Yes	5.83
	PDHG	3431	Yes	42.41
	GD	5000	No	61.31
10^{-3}	ALM-SSN-PCG	2/4/15	Yes	0.52
	ALM-SSN-CG	2/4/269	Yes	3.09
	PDHG	497	Yes	6.19
	GD	5000	No	60.72
10^{-2}	ALM-SSN-PCG	2/4/9	Yes	0.34
	ALM-SSN-CG	2/4/119	Yes	1.49
	PDHG	68	Yes	0.87
	GD	5000	No	62.19

Next, we compare new method with ALM-SSN-CG method for different mesh sizes. From Table 4, we observe that the convergence of ALM behaves mesh-independent. It should be noted that the iteration number of PCG method in the new algorithm is much less than that in ALM-SSN-CG method for all considered mesh sizes, which means the designed pre-conditioner is effective and robust to the mesh sizes. Furthermore, We notice that the iteration counts for both the SSN and PCG methods increase slightly as the mesh size becomes finer. However, this increase is marginal, and both remain relatively low. Consequently, the computational cost remains modest.

Table 4: Numerical comparison of our method with 'ALM-SSN-CG' with different mesh sizes for Example 2.

$(\Delta t, \Delta x)$	Method	#ALM	#SSN	#PCG	CPU(sec)
$(\frac{1}{20}, \frac{1}{40})$	ALM-SSN-PCG	3	6	405	3.44
	ALM-SSN-CG	3	30	2129	6.17
$(\frac{1}{40}, \frac{1}{80})$	ALM-SSN-PCG	2	4	103	6.56
	ALM-SSN-CG	2	8	680	25.92
$(\frac{1}{60}, \frac{1}{120})$	ALM-SSN-PCG	1	2	19	5.45
	ALM-SSN-CG	1	3	202	40.27
$(\frac{1}{80}, \frac{1}{160})$	ALM-SSN-PCG	1	2	15	13.29
	ALM-SSN-CG	1	3	199	120.90

Then, we recover the initial state and depict the obtained solution $\hat{u}_0^*$ and the corresponding final state by Figure 3. The initial source is also recovered accurately for this case. Besides, we consider the noisy observation u_T and compare the numerical solutions obtained from solving Problem (P) with a L^2 regularization parameter of $\tau = 10^{-5}$ against those obtained with $\tau = 0$. The numerical results are depicted in Figure 4. It's evident that the results obtained from Problem (P) with $\tau = 10^{-5}$ significantly outperform those obtained with $\tau = 0$.

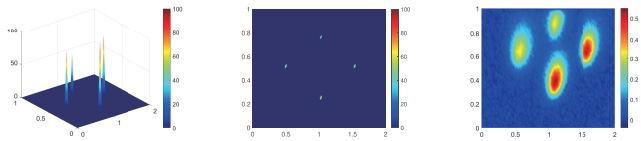

(a) Reference initial state (front view) (b) Reference initial state (above view) (c) Target u_T with noisy observation

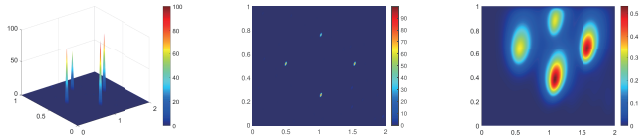

(d) Recovered initial state (front view) (e) Recovered initial state (above view) (f) Recovered final state

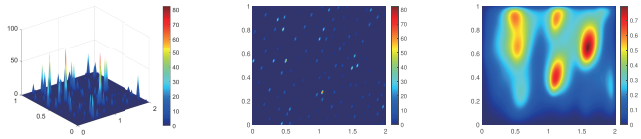

(g) Recovered initial state (front view) (h) Recovered initial state (above view) (i) Recovered final state

Figure 3: Source identification using new method for Example 2 with exact observation u_T.

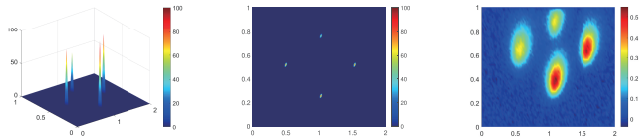

(a) Reference initial state (front view) (b) Reference initial state (above view) (c) Target u_T with noisy observation

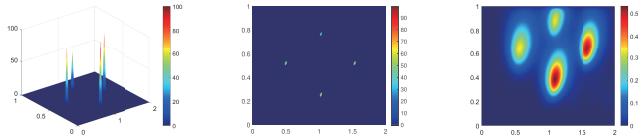

(d) Recovered initial state (front view) (e) Recovered initial state (above view) (f) Recovered final state

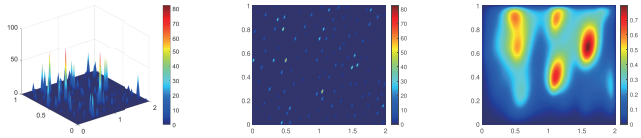

(g) Recovered initial state (front view) (h) Recovered initial state (above view) (i) Recovered final state

Figure 4: Source identification using new method for Example 2 with noisy observation u_T.

6.3 Example 3: initial source identification problem defined in coupled sense

The linear diffusion-advection equation (1.1) is modeled in a coupled sense. The space domain $\Omega = (0,2) \times (0,1)$ and the terminal time $T = 0.1$. The diffusivity coefficient $d = 0.05$ on Ω, and the advection vector $v = (0,0)^\top$ on $(0,1) \times (0,1)$ and $v = (0,-3)^\top$ on $(1,2) \times (0,1)$.

Similarly, four types of algorithms are used to solve the reformulated optimal control problem (P) and numerical results are listed in Table 5. From Table 5, it is clear that the convergence behavior of the ALM method is mesh-independent and the total iteration numbers of PCG/SSN method are small which validate that the designed pre-conditioner is also effective for this coupled model. Furthermore, the total computational cost of the new algorithm is cheap.

Table 5: Numerical results obtained by four methods with different τ for Example 3.

τ	Method	Iter	Convergence	CPU(sec)
10^{-5}	ALM-SSN-PCG	2/3/96	Yes	2.04
	ALM-SSN-CG	2/6/480	Yes	6.14
	PDHG	5000	No	61.93
	GD	5000	No	61.28
10^{-4}	ALM-SSN-PCG	2/4/62	Yes	1.44
	ALM-SSN-CG	2/5/390	Yes	4.62
	PDHG	3442	Yes	42.78
	GD	5000	No	60.41
10^{-3}	ALM-SSN-PCG	2/4/25	Yes	0.67
	ALM-SSN-CG	2/4/295	Yes	3.36
	PDHG	502	Yes	7.41
	GD	5000	No	61.12
10^{-2}	ALM-SSN-PCG	2/4/13	Yes	0.47
	ALM-SSN-CG	2/4/134	Yes	1.67
	PDHG	69	Yes	0.88
	GD	5000	No	61.91

Then, we compare Algorithm 5 with ALM-SSN-CG method with different mesh sizes and report the numerical results in Table 6. We observe that the convergence of ALM is mesh-independent. Besides, the number of iteration for the SSN method and PCG method does not increase greatly as the mesh size being finer, which further means the designed pre-conditioner is effective and robust to various mesh sizes even for coupled model.

Table 6: Numerical comparison of our method with ALM-SSN-CG method with different mesh sizes for Example 3.

$(\Delta t, \Delta x)$	Method	#ALM	#SSN	#PCG	CPU(sec)
$(\frac{1}{20}, \frac{1}{40})$	ALM-SSN-PCG	3	6	499	4.37
	ALM-SSN-CG	3	30	2445	7.35
$(\frac{1}{40}, \frac{1}{80})$	ALM-SSN-PCG	2	4	169	9.91
	ALM-SSN-CG	2	10	874	35.24
$(\frac{1}{60}, \frac{1}{120})$	ALM-SSN-PCG	1	2	35	9.12
	ALM-SSN-CG	1	4	299	58.21
$(\frac{1}{80}, \frac{1}{160})$	ALM-SSN-PCG	1	2	27	22.04
	ALM-SSN-CG	1	3	194	132.43

Finally, we recover the initial state and depict the obtained solution $\hat{u}_0^*$ and the corresponding final state by Figure 5. It can be observed that the initial source is also recovered accurately for this coupled model. Besides, we consider the noisy observation u_T and

compare the numerical solutions obtained by solving Problem (P) with L^2 regularization parameter $\tau = 10^{-5}$ with those obtained by solving Problem (P) with $\tau = 0$. The numerical results are depicted in Figure 6. We observe that the numerical results obtained by Problem (P) with $\tau = 10^{-5}$ is still much better than those obtained by Problem (P) with $\tau = 0$.

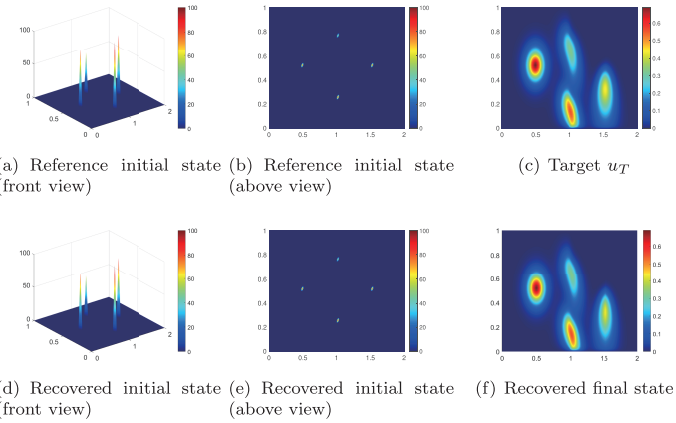

(a) Reference initial state (front view) (b) Reference initial state (above view) (c) Target u_T

(d) Recovered initial state (front view) (e) Recovered initial state (above view) (f) Recovered final state

Figure 5: Source identification using Algorithm 6 for Example 3 with exact observation u_T.

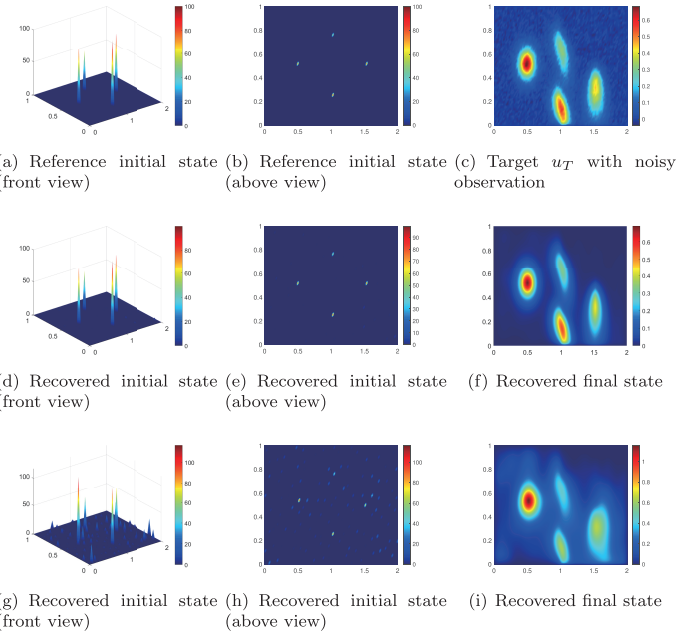

(a) Reference initial state (front view) (b) Reference initial state (above view) (c) Target u_T with noisy observation

(d) Recovered initial state (front view) (e) Recovered initial state (above view) (f) Recovered final state

(g) Recovered initial state (front view) (h) Recovered initial state (above view) (i) Recovered final state

Figure 6: Source identification using Algorithm 6 for Example 3 with noisy observation u_T.

7 Conclusion

In this paper, we considered the sparsity initial source identification of linear diffusion-advection equations. The initial source to be identified is a linear combination of Dirac measures indicating the locations, with the weights indicating the intensities. To tackle this

identification problem numerically, a two-stage algorithm is proposed. Firstly, we formulate an optimal control problem where the objective functional includes terms representing the discrepancy between the state at the terminal time and a predefined target function, along with L^1 and L^2 regularization terms. To efficiently solve this problem, we introduce an inexact augmented Lagrangian method (ALM), demonstrating its convergence properties and estimating its super-linear convergence rate. Additionally, we employ a semi-smooth Newton method (SSN) to handle each ALM sub-problem and design a preconditioned conjugate gradient method (PCG) for solving the resulting Newton system in each SSN iteration. This leads to the development of an ALM-SSN-PCG approach for solving the reformulated optimal control problem. In the second stage, we devise a procedure for identifying the locations of the sources, coupled with solving a least squares fitting problem to refine the solution obtained in the first stage. Through extensive experimentation, including scenarios involving homogeneous and heterogeneous media, coupled models, and noisy observations, we demonstrate the efficiency and accuracy of our proposed two-stage methodology.

References

[1] A. E. Badia, T. H. Duong and A. Hamdi, Identification of a point source in a linear advection–dispersion–reaction equation: application to a pollution source problem, *Inverse Probl.* 21 (2005): 1121.

[2] E. Borgens, C. Kanzow and D. Steck, Local and global analysis of multiplier methods for constrained optimization in Banach spaces, *SIAM J. Control Optim.* 57 (2019) 3694–3722.

[3] K. Bredies and H. Pikkarainen, Inverse problems in spaces of measures, *ESAIM: Control Optim. Calc. Var.* 19 (2013) 190–218.

[4] U. Biccari, Y. Song, X. Yuan and E. Zuazua, A two-stage numerical approach for the sparse initial source identification of a diffusion-advection equation, *Inverse Probl.* 39 (2023): 095003.

[5] E. Casas, C. Clason and K. Kunisch, Approximation of elliptic control problems in measure spaces with sparse solutions, *SIAM J. Control Optim.* 50 (2012) 1735–1752.

[6] E. Casas, C. Clason and K. Kunisch, Parabolic control problems in measure spaces with sparse solutions, *SIAM J. Control Optim.* 51 (2013) 28–63.

[7] C. Clason and K. Kunisch, A duality-based approach to elliptic control problems in nonreflexive Banach spaces, *ESAIM Control Optim. Calc. Var.* 17 (2011) 243–266.

[8] E. Casas and K. Kunisch, Using sparse control methods to identify sources in linear diffusion-convection equations, *Inverse Probl.* 35 (2019): 11402.

[9] P. Ciais, P. Rayner, F. Chevallier, P. Bousquet, M. Logan M, P. Peylin and M. Ramonet, Atmospheric inversions for estimating CO2 fluxes: methods and perspectives, *Clim. Change.* 103 (2010) 69–92.

[10] C. Clason and A. Schiela, Optimal control of elliptic equations with positive measures, *ESAIM Control Optim. Calc. Var.* 23 (2017) 217–240.

[11] E. Casas, B. Vexler and E. Zuazua, Sparse initial data identification for parabolic PDE and its finite element approximations, *Math. Control. Relat. Fields.* 5 (2016) 377–399.

[12] I. G. Enting, *Inverse Problems in Atmospheric Constituent Transport*, Cambridge University Press, Cambridge, 2002.

[13] J. Eckstein and P.J.S Silva, A practical relative error criterion for augmented Lagrangians, *Math. Program.* 141 (2013) 319–348.

[14] G. Gurarslan and H. Karahan, Solving inverse problems of groundwater pollution-source identification using a differential evolution algorithm, *Hydrogeology Journal.* 23 (2015) 1109–1119.

[15] R. Glowinski, J.L. Lions and J. He, Exact and Approximate Controllability for Distributed Parameter Systems: A Numerical Approach, Encyclopedia of Mathematics and its Applications,vol. 117, Cambridge University Press, Cambridge, 2008.

[16] M. Hinze, R. Pinnau, M. Ulbrich and S. Ulbrich, *Optimization with PDE Constraints*, Mathematical Modelling: Theory and Applications, vol. 23, Springer, New York, 2009.

[17] V. Isakov, *Inverse Problems for Partial Differential Equations*, Applied Mathematical Sciences, Spring, New York, third ed., 2017.

[18] L. Justen and R. Ramlau, A general framework for soft-shrinkage with applications to blind deconvolution and wavelet denoising, *Appl. Comput. Harmon. Anal.* 26 (2009) 43–63.

[19] K. Kunisch, K. Pieper and B. Vexler, Measure valued directional sparsity for parabolic optimal control problems, *SIAM J. Control Optim.* 52 (2014) 3078–3108.

[20] C. Kanzow, D. Steck and D. Wachsmuth, An augmented Lagrangian method for optimization problems in Banach spaces, *SIAM J. Control Optim.* 56 (2018) 272–291.

[21] G.S. Li, Y.J. Tan, J. Cheng and X.Q Wang, Determining magnitude of groundwater pollution sources by data compatibility analysis, *Inverse Probl. Sci. Eng.* 14 (2006) 287–300.

[22] D. Leykekhman, B. Vexler and D. Walter, Numerical analysis of sparse initial data identification for parabolic problems, *ESAIM Math. Model. Numer. Anal.* 54 (2020) 1139-1180.

[23] A. Mamonov and Y.H. Tsai, Point source identification in nonlinear advection-diffusion-reaction systems, *Inverse Probl.* 29 (2013): 035009.

[24] A. Monge and E. Zuazua, Sparse source identification of linear diffusion-advection equations by adjoint methods, *Syst. Control Lett.* 145 (2020): 104801.

[25] Y. Nesterov, *Lectures on Convex Optimization*, Springer Optimization and Its Applications, vol. 137, Springer, Cham, 2018.

[26] M.J.D. Powell, Algorithms for nonlinear constraints that use Lagrangian functions, *Math. Programming* 14 (1978) 224–248.

[27] M. Porcelli, V. Simoncini and M. Stoll, Preconditioning PDE-constrained optimization with L1-sparsity and control constraints, *Comput. Math. Appl.* 74 (2017) 1059–1075.

[28] M. Porcelli, V. Simoncini, M. Tani, Preconditioning of active-set Newton methods for PDE-constrained optimal control problems, *SIAM J. Sci. Comput.* 37 (2015) S472–S502.

[29] J.W. Pearson and A.J. Wathen, A new approximation of the Schur complement in preconditioners for PDE-constrained optimization, *Numer. Linear Algebra Appl.* 19 (2012) 816–829.

[30] R.T. Rockafellar, Monotone operators and augmented Lagrangian methods in nonlinear programming, in: *Nonlinear Programming, 3 (Proc. Sympos., Special Interest Group Math. Programming, Univ. Wisconsin, Madison, Wis., 1977)*, 1978, pp. 1–25.

[31] A. Rösch and G. Wachsmuth, Mass lumping for the optimal control of elliptic partial differential equations, *SIAM J. Numer. Anal.* 55 (2017) 1412–1436.

[32] Y. Sadd, On the rates of convergence of the Lanczos and the block-Lanczos methods, *SIAM J. Numer. Anal.* 17 (1980) 687–706.

[33] G. Stadler, Elliptic optimal control problems with L1-control cost and applications for the placement of control devices, *Comput. Optim. Appl.* 44 (2009) 159–181.

[34] Y. Saad, *Iterative Methods for Sparse Linear Systems*, Society for Industrial and Applied Mathematics, Philadelphia, PA, second edition, 2003.

[35] V. Thomée, *Galerkin Finite Element Methods for Parabolic Problems, volume 25 of Springer Series in Computational Mathematics*, Springer,Verlag, Berlin, second edition, 2006.

[36] H. Wang, C. Yu, and D. Wu, A duality-based approach for solving linear parabolic control constrained optimal control problems, *Optim. Contr. Appl. Met.* DOI: 10.1002/oca.3094, 2023.

Manuscript received 30 March 2024
revised 28 August 2024
accepted for publication 11 September 2024

Hailing Wang
Department of Mathematics, Shanghai University
Shanghai 200444, China
E-mail address: wanghailingshu@163.com

Hansong Yan
Shanghai University, Shanghai 200444, China
E-mail address: hansongyan@163.com

Di Wu
School of Mathematics, Physics and Statistics
Shanghai University of Engineering Science
Shanghai 201620, China
E-mail address: rosemary_di@163.com

Yanqin Bai
Department of Mathematics
Shanghai University, Shanghai 200444, China
E-mail address: yqbai@shu.edu.cn